Enhancement of the damping behavior of Ti6Al4V alloy through the use of trabecular structure produced by selective laser melting

J. Fiocchi[1], C.A. Biffi[1*], D. Scaccabarozzi[2], B. Saggin[2], A. Tuissi[1]

[1]National Research Council; Institute of Condensed Matter Chemistry and Technologies for Energy, Via Previati 1/E, 23900 Lecco, Italy.

[2] Politecnico di Milano, Department of Mechanical Engineering, Via Previati 1/C 23900 Lecco, Italy

[*]Corresponding author: carloalberto.biffi@cnr.it

Abstract

The interest of manufacturing complex devices is steadily growing for high technological application fields, such as the aerospace and biomedical ones, thanks to the possibility of coupling structural and functional properties. Additive Manufacturing (AM) allows to produce 3D complex geometries, like lattice structures, offering lightness together with good mechanical properties.

In the present work static and dynamic mechanical properties of Ti6Al4V lattice structures, produced by Selective Laser Melting, were investigated and compared with fully dense material, as reference. In details, the effects of heat treatment on mechanical properties and damping performance were investigated through tensile testing and dynamic compression measurements at different excitation frequencies and deformation amplitudes. The lattice structure can express a damping capacity of an order of magnitude higher than the full dense material, correlated to good mechanical behavior. In the prospective of newly designed parts for vibration suppression in aerospace applications, the opportunity of enhancing damping behavior by means of light structural components is allowed by the use of lattice structures.

Keywords

Selective laser melting; Titanium alloys; Mechanical properties; Damping; Lattice structure, space applications.

Introduction

Aerospace, Space and transport industries are increasingly asking for the employment of lightweight metallic structures, among which cellular materials are particularly interesting [1-2]. In the class of cellular materials the large degree of porosity induces two distinct effects, which allow promising use of these structures in different fields. In the view of a structural application, an elastic modulus and yield stress lower than the ones of the bulk solid are induced by the presence of porosity. Moreover, these mechanical properties may be tuned by varying the bulk – porosity ratio. On the other side, under compressive stress field these structures can reach particularly large deformations before the full densification is achieved, making them ideal materials for energy absorption during shock mitigation of impacts [1] or as interface dampers to reduce transmitted vibration to sensitive payloads onboard satellites during launch or operational phases [3-4]. . Beside internal friction and dislocation motion, the bending and buckling of the struts further increase the material damping ability. In recent years the rapid development of Additive Manufacturing (AM) technologies has spread the possibility of realizing cellular materials with regular structure, commonly named trabecular or lattice structures [5-7].

Among AM, selective laser melting (SLM) and electron beam melting (EBM) are based on the local melting of metallic powder bed using a laser beam and an electron beam, respectively [8-9]. The mechanical performances of the built materials are much higher than the conventionally casted ones, thanks to finer microstructures induced by rapid cooling rates [8]. The SLM process has been used for printing periodical lattice or hierarchical honeycomb structures in different alloys, like titanium, aluminum and stainless steel, and for achieving different aims, such as bone replacement, heat transfer and energy absorption or only for weight reduction purposes [10-16]. On the contrary, the EBM process has been adopted mainly for manufacturing lattice structure in Ti6Al4V alloy for biomedical applications, as the vacuum inside the EBM chamber permits to achieve high purity parts with limited oxygen concentrations [17-19].

Additionally to the previously mentioned performances, few works in literature have demonstrated that lattice structure can integrate another feature, which is important for aerospace and space sectors, i.e. a damping capacity significantly higher than the one of the full dense part [14,20].

In particular, Rosa et al. studied the damping behavior of 316L periodical lattice structures, produced by SLM with building orientation parallel to the platform, in the as built condition: the testing was done in high nominal plastic deformation condition [14]. In this respect, no studies regarding the damping behavior in elastic filed of SLMed lattice structure are available in the literature.

The choice of Ti6Al4V alloy for manufacturing lattice based components may favour their diffusion to other sectors, including the aerospace one, requiring relevant properties, like high mechanical properties, lightness, low thermal conductivity (wrt aluminum alloys)and excellent corrosion resistance [21]. All these properties are, in fact, offered by titanium alloys. Moreover, wrought titanium alloys have been already investigated for energy absorption applications and the effect of operating temperature and heat treatment on damping properties has been studied in literature [22-25].

Thanks to the finer microstructure obtained through the rapid cooling during the SLM process and the possibility of reproducing trabecular parts, the present study has the goal of investigating the static and dynamic mechanical properties of Ti6Al4V lattice structures. Moreover, the effect of a stress relief heat treatment, suggested by the material supplier, was investigated and compared to the performances of the as built condition on both bulk and lattice parts. The principal achievements are that lattice structure can offer higher deformability than the fully dense material, providing enhancement of the damping behavior in the field of elastic deformations.

Experimental

Bulk and lattice samples were produced from commercial Ti6Al4V powder by means of a SLM system (mod. AM400 from Renishaw), equipped with a pulsed wave laser. The adopted process parameters are listed in Table 1. Figure 1 depicts the schematic of the lattice structure, which is based on a tetragonal diamond-like structure (strut diameter and length of 1 mm and 2,5 mm, respectively). It has 18.5% of relative density with respect to full dense parts. The manufactured samples were prismatic lattice structures (10 mm x 100 mm x 30 mm), standard dog-bone specimens and laminas (80 mm x 20 mm x 1 mm), both having a thickness similar to the one of the lattice strut, for mechanical and damping testing. SLM samples were

built along the building direction (z axis) and tested in as built condition (AB) and after heat treatment (HT) at 850 °C for 2 h in vacuum, as suggested by the powder supplier for stress relieving. Before testing samples were washed with ultrasounds in acetone in order to remove loose powder. However, during optical microscopy inspection, some partially sintered powder particles were found to be attached to the struts.

Table 1: Process parameters used for the printing of the bulk and lattice samples

Power	Exposure time	Layer thickness	Point / hatch distance	Platform temperature	Atmosphere
100W	60µs	30µm	75µm	30°C	Argon

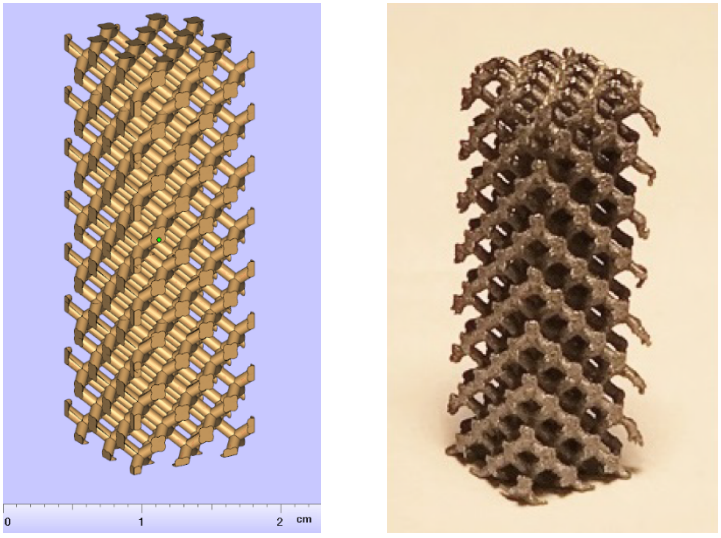

(a) (b)

Figure 1: 3D model (a) and picture (b) of the lattice structure produced by SLM

Morphological analysis was carried out using optical microscopy (Leitz Aristomet) on samples etched in Kroll's reagent. Quasi-static mechanical properties were evaluated by tensile testing with an MTS 2/M machine (strain rate of 0.015 min-1). Engineering stress and strain were computed considering the nominal section and length of the whole trabecular structure, as if it were a dense part, in order to highlight the differences with respect to the bulk samples [26].

Dynamic mechanical analysis (DMA) was used to evaluate the material loss factor by measuring complex modulus and loss factor of the lattice structures. Adopted testing setup comprises Bruel&Kjaier

electrodynamic shaker (V830 model) to apply force and displacement, Futek LTH300 donut load cell and DC-15 LVDT displacement sensors. More details about testing setup can be found in references [27-28]. The sample was subjected to a dynamic load, resulting in a phase lag δ between applied stress (amplitude σ_0) and the sample strain (ε_0). Stress σ and stain ε are linked together by the complex modulus:

$$\sigma = (E' + i\,E'')\varepsilon \qquad (1)$$

The real part E' is called "storage modulus", similar to the elastic one, while the imaginary part E'' is called "loss modulus", linked to energy dissipation and therefore damping.

By rearranging the terms in Equation (1), an ellipse in the stress-strain plane is obtained, providing a hysteresis loop whose area is related to the dissipated energy at each cycle:

$$\sigma = E'\,\varepsilon \pm E''\sqrt{\varepsilon_0^2 - \varepsilon^2} \qquad (2)$$

Dimensions of the ellipse are related to the storage and loss moduli therefore, these values can be used to estimate the material damping by computing the loss factor $\tan(\delta)$ as:

$$\tan(\delta) = \frac{E''}{E'} \qquad (3)$$

The testing was conducted with amplitude of the imposed deformation set equal to 0.1% and 0.45% and frequency to 30, 40 and 60 Hz. A preload of 900 N was applied to the sample in all tested conditions. As term for comparison, bulk material was tested by means of sonic resonance method [29] on two thin laminas. In that case, the loss factor was measured using well known half power method.

Analysis of Results and Discussion

The tensile testing was performed on lattice samples and the resulting mechanical properties were compared with the ones of the full dense alloy. The mechanical testing was performed on lattice samples and the tensile properties were compared with the ones of the full dense alloy. Figure 2 shows the stress strain curves of the samples. The curves of the as built and heat treated lattice samples show a linear elastic

behavior up to yielding, occurring at 34 MPa and 31 MPa respectively, followed by plastic deformation until failure (about 47 MPa). As expected, trabecular structures are characterized by much lower stiffness and mechanical resistance than corresponding bulk samples and the elongation to failure is largely higher in trabecular samples. Table 2 reports the values of the main mechanical features of the lattice and bulk samples. The heat treatment influences the ultimate tensile stress but not the yield stress in the bulk samples; on the contrary, no significant variations are detected in the lattice structures.

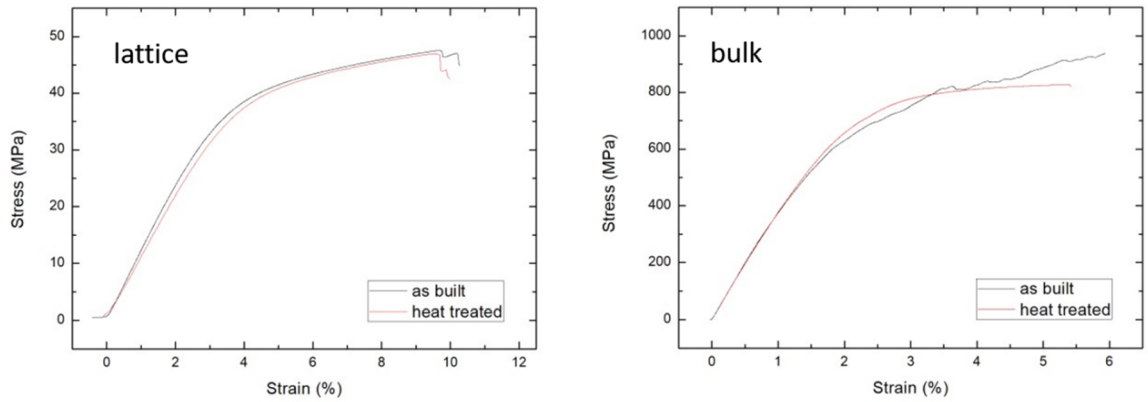

Figure 2: Stress-strain curves of trabecular (left) and full dense (right) samples in AB and HT conditions

Samples	E (MPa)	YS (MPa)	UTS (MPa)	Ef (%)
Bulk AB	38439 ± 125	542,3 ± 51	938,3 ± 62	5,9 ± 0,7
Bulk HT	39485 ± 432	621,6 ± 43	826,9 ± 24	5,4 ± 0,4
Lattice AB	1148 ± 3	34,1 ± 0,4	47,6 ± 0,7	10,7 ± 1
Lattice HT	1108 ± 5	31 ± 0,8	47,8 ± 1	11,9 ± 0,9

Table 2: Tensile properties of bulk and trabecular samples in as built and heat treated conditions

Dynamical characterization under low applied stress in compression was performed on lattice samples for evaluating their damping capacity without significant plastic deformation. Figure 3a shows the stress/strain loop of the lattice structure. The stress varied in the range ±6MPa while the strain in the range ±0.45%. The area contained inside the loop provides information about damping capacity of the structure.

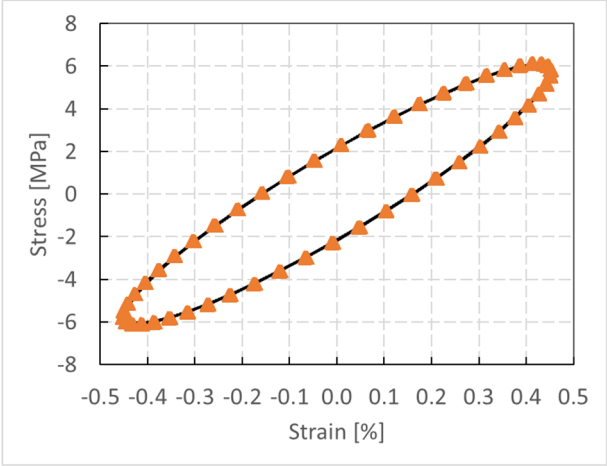

(a)

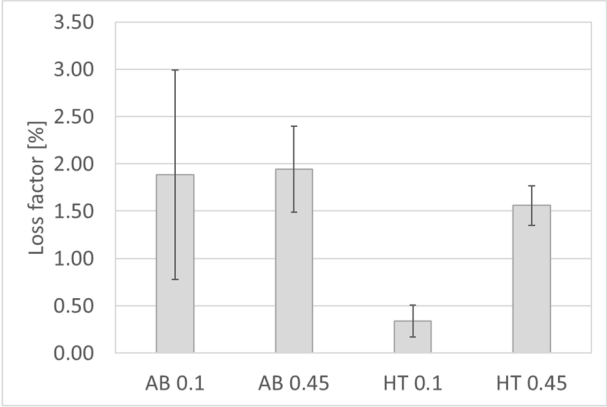

(b)

Figure 3: Passband filtered stress/strain loop (orange triangles) and optimized loop (black curve) of the lattice structure during DMA mechanical cycle (a); loss factors measured of lattice structures (b) for AB and HT conditions, depending on the applied deformation. In black line 1σ dispersion bands are shown.

Sample	Deformation amplitude 0.1%			Deformation amplitude 0.45%		
	30 Hz	40 Hz	60 Hz	30 Hz	40 Hz	60 Hz
Lattice AB	1.29	1.38	1.08	2.45	2.50	2.59
Lattice AB	3.33	3.53	3.18	1.87	1.71	1.89
Lattice AB	1.12	1.12	0.92	1.52	1.57	1.40
Lattice HT	0.14	0.18	0.10	1.46	1.46	1.42
Lattice HT	0.51	0.53	0.54	1.58	1.60	1.16
Lattice HT	0.32	0.37	0.35	1.81	1.75	1.79

Table 3: Measured loss factors (% units) for trabecular samples: frequency, heat treatment and amplitude dependence.

The measured loss factors for the lattice structures showed that achievable damping is between 0.5% and 2%. Analyzing the frequency behavior of the tested samples (see Table 3), it may be noticed that there is no significant dependence of the loss factor on the exciting frequency; this agrees with metallic foams behavior [18]. The tests on the lattice structures revealed noticeable variability in damping (especially for the AB samples), most likely caused by the non-homogeneous material distribution, making each sample different from the others. The weird behavior has not been identified in the HT samples that always show increasing of the loss factors with strain amplitude increase. Considering as a whole the measured loss factors average value of 1.6 10^{-2} for the maximum cyclic strain was achieved. The measurement variability (considering both the sample and manufacturing process) for the tested samples is about 9.2 %, caused by the intrinsic variability of the SLM process similarly to what was obtained with the as-produced structures. Moreover, the heat treatment affects the measured damping, since measured loss factors are lower than for AB samples and also measurement variability is reduced (see comparison in Figure 3b).

As term of comparison with respect to the lattice structures, dynamic tests were carried out on SLM built full dense laminas. The sample bulk samples were suspended by means of two strings to simulate unconstrained conditions. Frequency response function was used for evaluating the corresponding loss factor, as shown in Figure 4a [29]. The achievable damping of the bulk samples is two orders of magnitude lower than the one obtained with the lattice structures. This confirms that the open cell materials allow increasing the specific damping capacity.

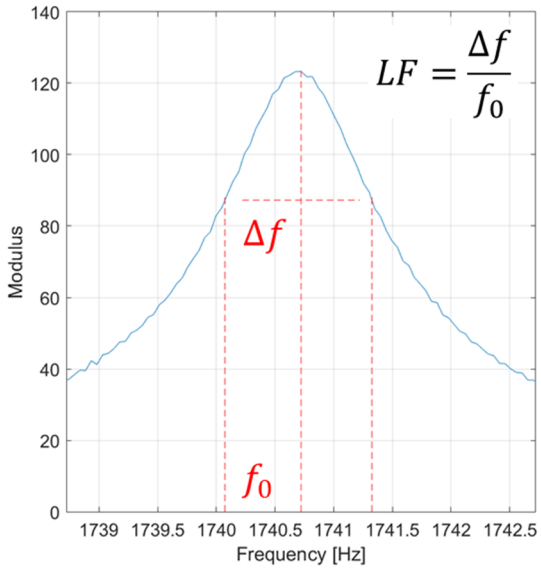

(a)

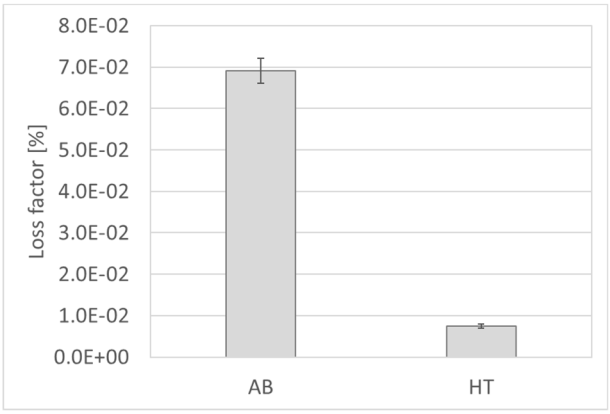

(b)

Figure 4: Frequency response function bulk sample, including the implementation of the half power method to measure the loss factor (a); loss factor measured for the bulk samples (b).

Representative microstructures of trabecular samples, depicting xy section before and after heat treatment, are shown in Figure 5a-b and c-d, respectively. The microstructure of as-built Ti6Al4V alloy is dominated by large prior β grains, highlighted by different gray shades in Figure 5a, which, because of an extremely high cooling rate during SLM, are completely transformed to martensitic α' phases. The α' acicular phase can be recognized in Figure 5b under the form of fine needles. After the heat treatment at 850 °C, which is below the β transus temperature, a lamellar α + β mixture is formed (Figure 5c-d). Grains are still visible and maintain roughly the same size. They consist of intercalated α (bright phase) and β (dark

phase) platelets. Moreover, grain boundaries are often characterized by a higher abundance of α phase, as visible in the top-right corner of Figure 5d.

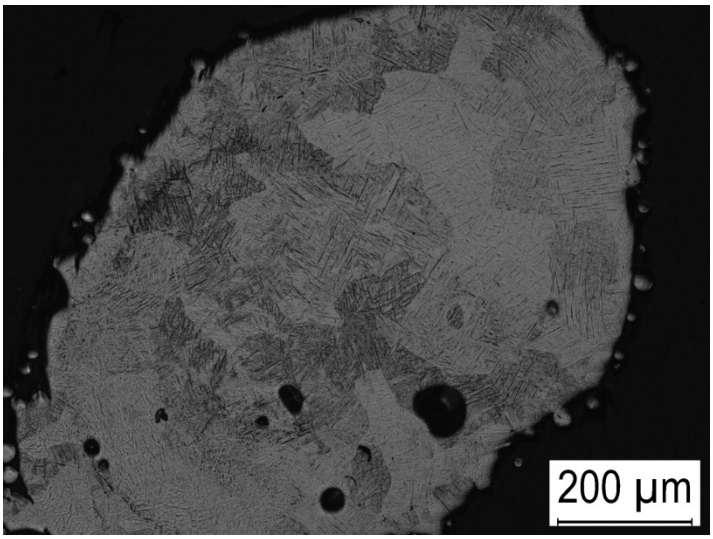

(a)

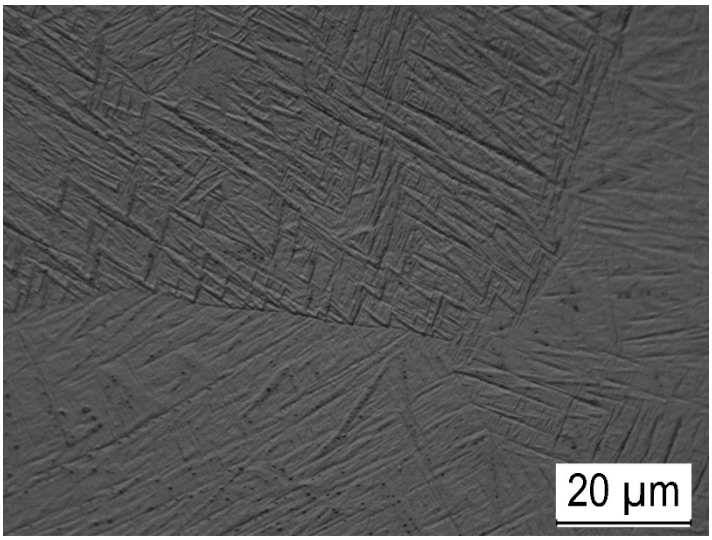

(b)

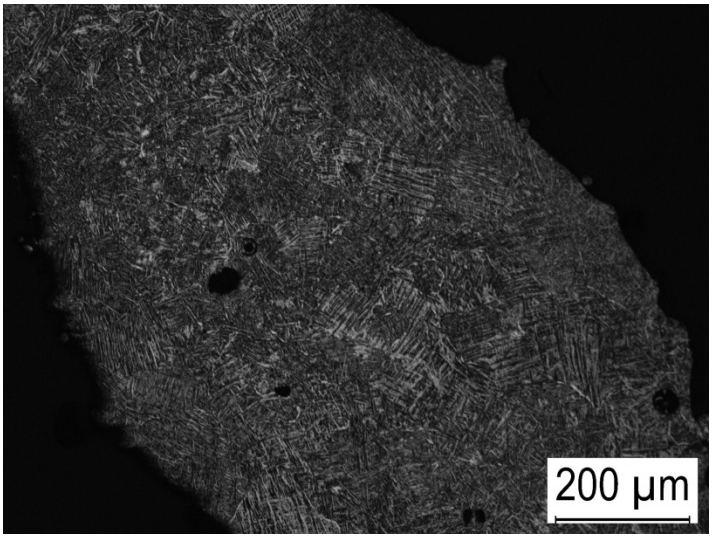

(c)

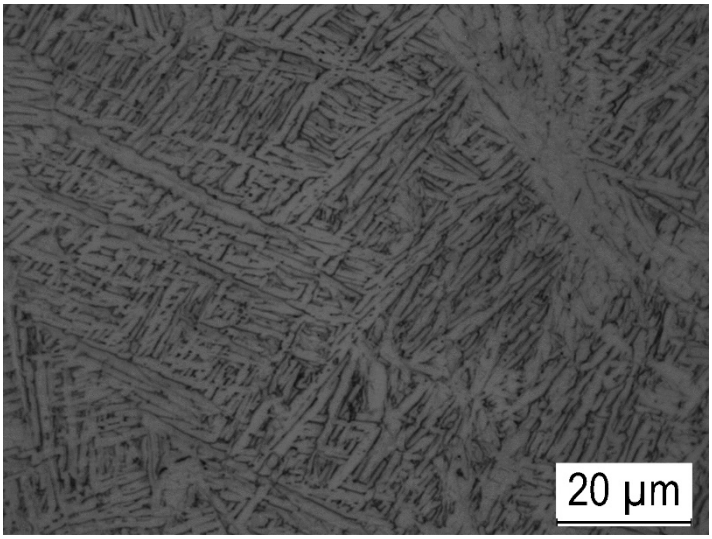

(d)

Figure 5: Microstructure of AB (a) and HT (b) TiAlV64 trabecular samples.

The high value of the damping coefficient in the as built condition (Figure 4b) is confirmed by the presence of β grains containing α' lamellar phase, able to induce the mechanisms of energy dissipation [22]. In fact, after quenching or rapid solidification occurring in SLM process the damping capacity can be increased by more than an order of magnitude when a meta-stable structure is generated.

An interpretation of the high damping is that the tension-compression oscillation causes structural reversal of metastable phase conditions in an anelastic way, thus dissipating elastic strain energy. The damping and the modulus values are mass-weighted averages of the contributions by the primary α phase and the second β, α" or α‘ phase: this microstructure consists of soft α phase and tempered martensite with

different stiffness, which has the same characteristics as a composite material, therefore shows higher damping properties compared with the other microstructures. On the contrary, Titanium alloys with stable α+β phase mixtures have low damping capacity. This can explain the reason why the heat treatment limit the damping capacity, even if it can relief the residual stresses induced by the local rapid solidification of the SLM process.

Moreover, during the testing the stress distribution change from the bulk sample to the lattice one can promote an enhancing of the energy dissipation, due to stress concentration in the points of intersection among of single linear elements, constituting the trabecular structure.

Conclusions

Mechanical testing of Ti6Al4V lattice structures made by SLM confirmed the high potential of coupling structural and functional properties in lightweight components. In details, the lattice structures showed stable mechanical properties, enhanced deformation capability and high damping capacity for elastic deformation range. The measured damping capacity was found to be about two order of magnitude larger than the one displayed by bulk samples of the same material, even after the required heat treatment. The effect of the heat treatment on damping was correlated to a lowering effect, confirmed by previous literature studies. The obtained result would be very attractive for many different technological fields, and in particular for the Space and Aerospace sectors, where adoption of lattice-based parts would offer reasonable strength, lightness and enhanced damping capacity beside the powerful design freedom granted by additive manufacturing technologies.

Further investigation will be taken into account for studying the mechanisms of energy dissipation, associated to specific AMed microstructures, and numerical analysis of the stresses during the mechanical cycling will be considered in next works for optimizing the damping behavior with ad hoc heat treatments.

Acknowledgments

The authors would like to acknowledge Nicola Bennato from CNR-ICMATE and Riccardo Somaschini from Politecnico di Milano for their assistance in the experiments.

References

[1] L. Gong, S. Kyriakides, W.Y. Jang, Compressive response of open cell foams. Part I: Morphology and elastic properties, International Journal of Solids Structures 42 (2005) 1355–1379.

[2] W.M. Chen, Y.M. Xie, G. Imbalzano, J. Shen, S. Xu, S.J. Lee, P.V.S. Lee, Lattice Ti structures with low rigidity but compatible mechanical strength: Design of implant materials for trabecular bone, International Journal of Precision Engineering Manufacturing 17 (2016) 793–799.

[3] B. Saggin, D. Scaccabarozzi, L. Comolli, Long-term vibration monitoring onboard mars express mission, Journal of Spacecraft and Rockets 51.5 (2014) 1664-1672

[4] D. Scaccabarozzi, B. Saggin, E. Alberti, Design and testing of a roto-translational shutter mechanism for planetary operation, Acta Astronautica, 93 (2014) 207-216.

[5] E. Sallica-Leva, A.L. Jardini, J.B. Fogagnolo, Microstructure and mechanical behavior of porous Ti-6Al-4V parts obtained by selective laser melting, Journal of Mechanical Behaviour of Biomedical Materials 26 (2013) 98–108.

[6] S.Y. Choy, C.N. Sun, K.F. Leong, J. Wei, Compressive properties of Ti-6Al-4V lattice structures fabricated by selective laser melting: Design, orientation and density, Additive Manufacturing 16 (2017) 213–224.

[7] M. Pham, C. Liu, I. Todd, J. Lertthanasarn, Damage-tolerant architected materials inspired by crystal microstructure, Nature 565 (2019) 305- 311.

[8] L. E. Murr, S. M. Gaytan, D. A. Ramirez, E. Martinez, J. Hernandez, K. N. Amato, P. W. Shindo, F. R. Medina, R. B. Wicker, Metal Fabrication by Additive Manufacturing Using Laser and Electron Beam Melting Technologies, Journal of Materials Science Technology, 2012, 28(1), 1–14.

[9] W.S.W. Harun, N.S. Manam, M.S. I.N. Kamariah, S. Sharif, A.H. Zulkifly, I. Ahmad, H. Miura, A review of powdered additive manufacturing techniques for Ti-6al-4v biomedical applications, Powder Technology 331 (2018) 74–97.

[10] Q. Feng, Q. Tang, Y. Liu, R. Setchi, S. Soe, S. Ma, L. Bai, Quasi-static analysis of mechanical properties of Ti6Al4V lattice structures manufactured using selective laser melting, International Journal of Advanced Manufacturing Technology (2017) 2301–2313.

[11] A.F. Obaton, J. Fain, M. Djemaï, D. Meinel, F. Léonard, E. Mahé, B. Lécuelle, J.J. Fouchet, G. Bruno, In vivo XCT bone characterization of lattice structured implants fabricated by additive manufacturing, Heliyon. 3 (2017) e00374.

[12] Qiu, C.; Yue, S.; Adkins, N.J.E.;Ward, M.; Hassanin, H.; Lee, P.D.;Withers, P.J.; Attallah, M.M. Influence of processing conditions on strut structure and compressive properties of cellular lattice structures fabricated by selective laser melting, Material Science and Engineering A 628 (2015) 188–197.

[13] Y. Zhang, T. Liu, H. Ren, I. Maskery, I. Ashcroft, Dynamic compressive response of additively manufactured AlSi10Mg alloy hierarchical honeycomb structures, Composite Structures 195 (2018) 45–59.

[14] F. Rosa, S. Manzoni, R. Casati, Damping behavior of 316L lattice structures produced by Selective Laser Melting, Materials and Design 160 (2018) 1010–1018.

[15] B. Van Hooreweder, K. Lietaert, B. Neirinck, N. Lippiatt, CoCr F75 scaffolds porduced by additive manufacturing: influence of chemical etching on powder removal and mechanical performance, Journla of Mechanical Behaviour of Biomedical Materials 70 (2017) 60-67.

[16] A.G. Demir, B. Previtali, Additive manufacturing of cardiovascular CoCr stents by selective laser

melting, Materials and Design 119 (2017) 338-350.

[17] X.Y.Cheng, S.J.Li, L.E.Murr, Z.B.Zhang, Y.L.Hao, R.Yang, F.Medina, R.B.Wicker, Compression deformation behavior of Ti–6Al–4V alloy with cellular structures fabricated by electron beam melting, Journal of the Mechanical Behaviour of Biomedical Materials 16 (2012) 153-162.

[18] X. Li, C. Wang, W. Zhang, Y. Li, Fabrication and characterization of porous Ti6Al4V parts for biomedical applications using electron beam melting process, Materials Letters 63 (2009) 403–405.

[19] Horn TJ, Harrysson OLA, Marcellin-Little DJ, West, HA, Lascelles BDX, Aman R, Flexural properties of ti6al4v rhombic dodecahedron open cellular structures fabricated with electron beam melting, Additive Manufacturing 1-4 (2014) 2-11.

[20] R. Ramadani, A. Belsak, M. Kegl, J. Predan, S. Pehan, Topology optimization based design of lightweight and low vibration gear bodies, International Journal of Simulation Modelling 17 (1) (2018) 92–104.

[21] E.O. Ezugwu, Z.M. Wang, Titanium alloys and their machinability, Journal of Materials Processing Technololgy 68 (1997) 262–274.

[22] Y.T. Lee, G. Welsch, Young's Modulus and Damping of Ti-6AI-4V Alloy as a Function of Heat Treatment and Oxygen Concentration, Materials Science and Engineering A 128 (1990) 77–89.

[23] P. Deodati, R. Donnini, R. Montanari, C. Testani, High temperature damping behaviour of Ti6Al4V – SiC f composite, Materials Science and Engineering A 522 (2009) 318–321.

[24] A. Kumar, S. Omer, Young ’ s modulus and damping in dependence on temperature of Ti – 6Al – 4V components fabricated by shaped metal deposition, Journal of Materials Science (2011) 3802–3811.

[25] S. Amadori, E. Bonetti, L. Pasquini, P. Deodati, R. Donnini, R. Montanari, C. Testani, Low temperature anelasticity in Ti6Al4V alloy and Ti6Al4V–SiC composite, Materials Science and Engineering A 522 (2009) 340–342.

[26] Ashby, M. F., Evans, T., Fleck, N. A., Hutchinson, J. W., Wadley, H. N. G., & Gibson, L. J., Metal foams: a design guide. Elsevier (2000).

[27] D. Scaccabarozzi, B. Saggin, M. Magni, A. Sesana, M. Tarabini, J. Fiocchi, C. A. Biffi, A. Tuissi, Specific Damping Capacity of CuZn and CuZnAl Metal Foams, a Preliminary Study, 5th IEEE International Workshop on Metrology for AeroSpace (MetroAeroSpace)(2018) 500-505.

[28] Scaccabarozzi, D., Saggin, B., Valiesfahani, A., Biffi, C. A., & Tuissi, A. (2017, June). Feasibility design of an interface damper for a space borne microbalance. In Metrology for AeroSpace (MetroAeroSpace), 2017 IEEE International Workshop on (pp. 439-444).

[29] ASTM E1875-13 Standard Test Method for Dynamic Young’s Modulus, Shear Modulus, and Poisson’s Ratio by Sonic Excitation.